

Smart Grid Technologies for Reactive Power Compensation in Motor Start Applications

Maryclaire Peterson, *Member, IEEE* and Brij N. Singh, *Member, IEEE*

Abstract—Several major power outages have been attributed to insufficient voltage support and subsequent voltage collapse. Accordingly, reactive power management has gained increased attention for reliability maintenance of both transmission and distribution systems. In particular, motor starting applications draw a large amount of reactive power and contribute to system degradation, particularly in a weak area. Consequently, this paper investigates smart grid technologies for reactive power compensation for motor starting applications in order to provide the necessary voltage support, reduce the inrush current, and decrease the motor starting time. The two dynamic VAR devices that are proposed are the Static Compensator (STATCOM) and Static Synchronous Series Compensator (SSSC). Detailed mathematical models are developed for these devices as well as the proposed control logic. Simulation results for STATCOM and SSSC-based compensators are provided to verify the accuracy of the developed models and control logic and observe the effectiveness of the dynamic VAR devices.

Index Terms—Reactive power, Static compensators, Static synchronous series compensators.

I. INTRODUCTION

Reactive power compensation is essential for satisfactory performance and reliable operation of AC power systems. Inadequate reactive power support leads to unacceptable system voltages and reduced ability to transfer power from source to load. Under extreme conditions, insufficient VAR support may contribute to voltage collapse and wide-area blackouts. Appropriate reactive power compensation techniques provide such benefits as increased transmission efficiency through reduced losses, reduced grid congestion, increased transfer capability, and enhanced grid reliability [1].

Reactive power compensation technologies are divided into two broad categories: static VAR compensation and dynamic VAR compensation. Static VAR devices are the most cost-effective; however, their primary constraint is that their reactive power output is dependent on the square of the system voltage. Consequently, adequate reactive power compensation may not be available when it is needed most at lower system voltages. Dynamic VAR devices are “smart technologies”, which can be utilized to provide fast reactive power support despite low voltage conditions.

This paper demonstrates the effectiveness of two “smart

technologies” for reactive power compensation required for a common low voltage scenario, the direct on-line starting of an induction motor. An uncontrolled starting of an induction motor draws six to seven times the rated current, resulting in an unacceptable voltage sag in the AC power system. Voltage sags contribute to the malfunctioning of very sensitive equipment at the PCC [2]. Moreover, the voltage sag during the DOL starting of a high power induction motor could be further prolonged due to an increased starting time. Lengthy starting times are caused from a substantial reduction in the starting torque under a reduced voltage available at the motor terminals.

The dynamic VAR devices discussed in this paper are the Static Compensator (STATCOM) and Static Synchronous Series Compensator (SSSC). The mathematical models and control logic for the STATCOM and SSSC are developed and converted to simulation models, which are used to demonstrate their dynamic and steady-state performance.

II. MATHEMATICAL MODEL AND CONTROL LOGIC OF THE STATCOM

Fig. 1 shows the schematic for the shunt compensated inductor motor utilizing a static compensator (STATCOM), a dynamic VAR device. The STATCOM is desirable because it not only instantaneously compensates reactive power at the PCC but also is capable of suppressing current harmonics and eliminating unbalance in the supply voltages [3-5]. For STATCOM configurations, reactive power compensation is provided by a current-controlled voltage source inverter (CC-VSI) connected in parallel to the power system. The CC-VSI has a self-supported DC bus that allows it to supply the desired reactive power at the PCC.

The switching devices of the active filter are controlled using the indirect current control technique based on reactive power theory [6]. The actual load currents ($i_{La,Lb,Lc}$) and the PCC voltages ($v_{pcca,b,c}$) are sensed and transformed into the α - β frame to compute the instantaneous value of real (p) and reactive (q) powers consumed by the load.

A. Mathematical Model of STATCOM

In Fig. 1, the schematic of the STATCOM is enclosed in the dashed box. The STATCOM circuit can be represented by the following mathematical equations.

$$v_{sa, sb, sc} = R_c i_{ca, cb, cc} + L_c \frac{di_{ca, cb, cc}}{dt} + e_{a, b, c} \quad (1)$$

where, $v_{sa, sb, sc}$ are the three-phase voltages at the PCC, $i_{ca, cb, cc}$

Maryclaire Peterson is with Entergy Services, Inc., New Orleans, LA 70113 USA (e-mail: mpeter2@entergy.com).

are the three-phase output currents from the STATCOM, and $e_{a,b,c}$ are the three-phase PWM voltages at the STATCOM pole points a , b , and c . The parameters R_c and L_c are the per-phase STATCOM resistance and inductance, respectively.

The PWM voltages at the STATCOM pole points are expressed in terms of the STATCOM DC bus voltage and the switching states (SA, SB, SC) as follows:

$$\begin{aligned} e_a &= \frac{v_{dc}}{3}(2SA - SB - SC) \\ e_b &= \frac{v_{dc}}{3}(-SA + 2SB - SC) \\ e_c &= \frac{v_{dc}}{3}(-SA - SB + 2SC) \end{aligned} \quad (2)$$

On the DC side, the current (i_{dc}) through the capacitor is expressed as:

$$i_{dc} = C_{dc} \frac{dv_{dc}}{dt} \quad (3)$$

where, v_{dc} is the voltage across the capacitor. The capacitor current (i_{dc}) can be expressed in terms of the inverter input current (i_c) and current through resistor R_L (i_L) as in Equation (4).

$$i_{dc} = i_c - i_L \quad (4)$$

The current i_L can be expressed in terms of the DC bus voltage as in Equation (5).

$$i_L = \frac{v_{dc}}{R_L} \quad (5)$$

The inverter input current (i_c) shown in Fig. 1 can be expressed in terms of the three output currents and the three switching states. The inverter input current (i_c) is expressed as:

$$i_c = (SA)i_{ca} + (SB)i_{cb} + (SC)i_{cc} \quad (6)$$

The derivative of the DC voltage can be expressed in its final form using Equations (3) through (6).

$$\frac{dv_{dc}}{dt} = \frac{(SA)}{C_{dc}}i_{ca} + \frac{(SB)}{C_{dc}}i_{cb} + \frac{(SC)}{C_{dc}}i_{cc} - \frac{v_{dc}}{R_L C_{dc}} \quad (7)$$

The feedback-based PWM current control scheme that is used to control the switching states (SA, SB, SC) and computation of the relevant reference currents (i_{ca}^* , i_{cb}^* , and i_{cc}^*) for the close loop control of the STATCOM currents ($i_{ca,cb,cc}$) is detailed in the next section. The mathematical simulation and sensor-less implementation of a real-time STATCOM system is carried out by solving the differential equations given in Equation (1). Once the STATCOM currents ($i_{ca,cb,cc}$) are computed, the voltages imposed across the induction motor terminals are expressed as:

$$v_{sa, sb, sc} = v_{an, bn, cn} - R_s i_{sa, sb, sc} - L_s \frac{di_{sa, sb, sc}}{dt} \quad (8)$$

Since the currents ($i_{La, Lb, Lc}$) at the input of the motor terminals are realized through the induction motor model, and the STATCOM currents ($i_{ca, cb, cc}$) are computed above, the supply currents ($i_{sa, sb, sc}$) and their derivatives can be derived in terms of these currents as in Equations (9) and (10).

$$i_{sa, sb, sc} = i_{La, Lb, Lc} - i_{ca, cb, cc} \quad (9)$$

$$\frac{di_{sa, sb, sc}}{dt} = \frac{di_{La, Lb, Lc}}{dt} - \frac{di_{ca, cb, cc}}{dt} \quad (10)$$

Consequently, the voltages imposed across the induction motor terminals are computed by substituting Equations (9) and (10) into Equation (8).

$$v_{sa, sb, sc} = v_{an, bn, cn} - R_s (i_{La, Lb, Lc} - i_{ca, cb, cc}) - L_s \left(\frac{di_{La, Lb, Lc}}{dt} - \frac{di_{ca, cb, cc}}{dt} \right) \quad (11)$$

B. Control Scheme of STATCOM

Prior to starting the motor, the DC bus capacitor is charged to obtain a desired voltage level across the inverter's DC bus.

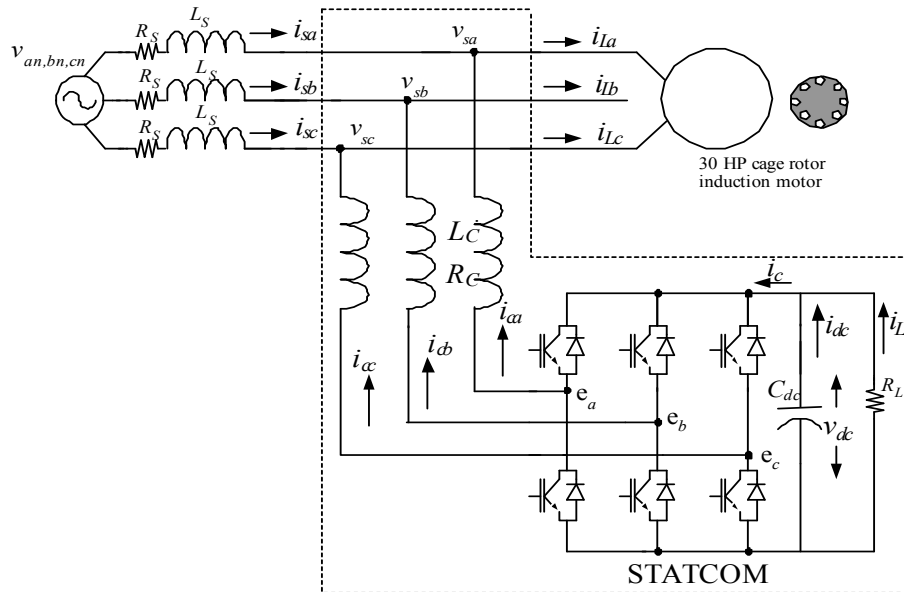


Fig. 1. Schematic of shunt compensated induction motor.

A PID controller is used to charge the DC bus capacitor and continues to monitor the voltage level of the inverter's DC bus in order to maintain the desired voltage required to avoid loss of current control and occurrence of current distortion.

The induction motor currents ($i_{La,Lb,Lc}$) and inverter currents ($i_{ca,cb,cc}$) are sensed, and the supply currents ($i_{sa,sb,sc}$) are computed by subtracting the inverter currents from the motor currents. The voltages imposed across the induction motor terminals ($v_{sa,sb,sc}$) are computed using the mathematical derivations described in the above section. The motor currents, supply currents, and motor terminal voltages are transformed into the α - β reference frame to compute the instantaneous value of the real (p) and reactive (q) powers consumed by the motor and supplied by the source. This computation is given in Equation (12).

$$\left. \begin{aligned} p_{sply} &= v_{s\alpha} \cdot i_{s\alpha} + v_{s\beta} \cdot i_{s\beta} \\ q_{sply} &= -v_{s\beta} \cdot i_{s\alpha} + v_{s\alpha} \cdot i_{s\beta} \\ p_{motor} &= v_{s\alpha} \cdot i_{L\alpha} + v_{s\beta} \cdot i_{L\beta} \\ q_{motor} &= -v_{s\beta} \cdot i_{L\alpha} + v_{s\alpha} \cdot i_{L\beta} \end{aligned} \right\} \quad (12)$$

The reactive power consumed by the motor should come partially from the STATCOM and partially from the supply system. However, to eliminate voltage sag at the PCC, it is preferred that the majority of the reactive power comes from the STATCOM. A PI controlled is used to control the reactive power output of the STATCOM. The required reactive power output (\bar{q}^*) is calculated from the difference between the motor side reactive power demand and the supply side reactive power. As shown in Equation (13), the STATCOM reference currents in the α - β frame ($i_{c\alpha}^*, i_{c\beta}^*$) are computed using the required reactive power output (\bar{q}^*) needed to be supplied by the STATCOM [6].

$$i_{c\alpha}^* = \frac{-v_{s\beta}}{v_{s\alpha}^2 + v_{s\beta}^2} \bar{q}^* \quad (13)$$

$$i_{c\beta}^* = \frac{v_{s\alpha}}{v_{s\alpha}^2 + v_{s\beta}^2} \bar{q}^*$$

The three-phase abc reference currents are obtained by the following expression:

$$\begin{bmatrix} i_{ca}^* \\ i_{cb}^* \\ i_{cc}^* \end{bmatrix} = \sqrt{\frac{2}{3}} \begin{bmatrix} 1 & 0 \\ -\frac{1}{2} & \frac{\sqrt{3}}{2} \\ -\frac{1}{2} & -\frac{\sqrt{3}}{2} \end{bmatrix} \begin{bmatrix} i_{c\alpha}^* \\ i_{c\beta}^* \end{bmatrix} \quad (14)$$

The reference ($i_{ca,cb,cc}^*$) and actual ($i_{ca,cb,cc}$) inverter currents are compared in a PWM current controller to generate the switching signals for the STATCOM device. This control technique results in a self-supporting DC bus of the STATCOM to feed the desired reactive power at the PCC.

III. MATHEMATICAL MODEL AND CONTROL LOGIC OF THE SSSC

Fig. 2 shows the schematic for the series compensated inductor motor utilizing a static synchronous series compensator (SSSC), a dynamic VAR device [7]. Contrary to the STATCOM, the SSSC is operated in voltage control mode, and therefore, a voltage-controlled voltage source inverter (VC-VSI) is used as the SSSC hardware. The SSSC injects three-phase voltages in series with the line connecting the induction motor with the supply system. For the SSSC, an energy storage device is used on the DC bus of the inverter to produce the desired (phase and magnitude) output voltages. The injected voltages are precisely controlled to allow full compensation at startup and only a needed compensation afterwards. The injected voltages compensate voltage sag resulting in a increased startup acceleration and substantially reduced starting time.

A. Mathematical Model of SSSC

Similar to the mathematical model of the STATCOM, the equations for the three-phase SSSC currents are obtained using the inverter circuit shown in the dashed box in Fig. 1. The SSSC circuit can be represented by following mathematical equations.

$$e_{a,b,c} = (R_c + R_t) i_{ca,cb,cc} + (L_c + L_t) \frac{di_{ca,cb,cc}}{dt} \quad (15)$$

where, $R_t = R_{ts} + R_{tp}$ is the injection transformer windings' resistance and $L_t = L_{ts} + L_{tp}$ is the injection transformer windings' leakage inductance. The quantities ($e_{a,b,c}$) are the inverter (SSSC power converter) pole voltages, which are computed as per Equation (2). The three-phase output currents of the SSSC are obtained by solving the differential equations in Equation (15). Consequently, the three-phase voltages imposed across the induction motor terminals (Fig. 2) are computed from the three-phase SSSC output currents. As shown in Equation (16), for series compensation, the injected voltage vectors produced by the SSSC are added with the supply voltage vectors, resulting in compensation of the desired reactive power.

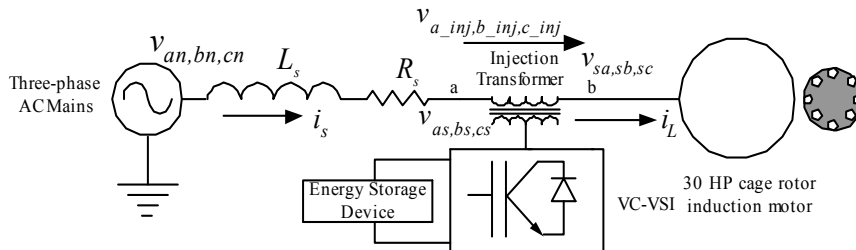


Fig. 2. Single line diagram of an active series compensated induction motor.

$$v_{sa, sb, sc} = v_{an, bn, cn} - R_s i_{sa, sb, sc} - L_s \frac{di_{sa, sb, sc}}{dt} + v_{a, b, c_inj} \quad (16)$$

The injected voltages (v_{a_inj, b_inj, c_inj}) imposed on the injection transformer primary (Fig. 2) are realized by the voltage control of the SSSC power circuit. The mathematical relationship between the injected voltages and inverter currents are given in Equation (17).

$$v_{a, b, c_inj} = (R_{ts} + R_{tp}) i_{ca, cb, cc} + (L_{ts} + L_{tp}) \frac{di_{ca, cb, cc}}{dt} \quad (17)$$

The scheme used to control the switching states (SA, SB, SC) and injected voltages is described the next section.

B. Control Scheme of SSSC

Unlike shunt compensation, the SSSC system requires a constant DC bus voltage, which is ensured by using a 150V DC supply to feed power to SSSC DC bus.

The induction motor currents ($i_{La, Lb, Lc}$) are sensed, and the voltages appearing at both sides ($(v_{as, bs, cs})$ and $(v_{sa, sb, sc})$) of the injection transformer are computed to determine the real (p) and reactive (q) powers consumed by the motor and fed by the supply system. The difference between the reactive power consumed by the motor and supplied by the source is produce by the SSSC. The instantaneous value of real (p) and reactive (q) powers consumed by the motor and supplied by the source are expressed in Equation (18).

$$\left. \begin{aligned} p_{sply} &= v_{\alpha s} \cdot i_{L\alpha} + v_{\beta s} \cdot i_{L\beta} \\ q_{sply} &= -v_{\beta s} \cdot i_{L\alpha} + v_{\alpha s} \cdot i_{L\beta} \end{aligned} \right\} \quad (18)$$

$$\left. \begin{aligned} p_{motor} &= v_{s\alpha} \cdot i_{L\alpha} + v_{s\beta} \cdot i_{L\beta} \\ q_{motor} &= -v_{s\beta} \cdot i_{L\alpha} + v_{s\alpha} \cdot i_{L\beta} \end{aligned} \right\}$$

To eliminate voltage sag at the PCC, it is preferred that the majority of the reactive power consumed by the motor be produced by the SSSC via a PI controller based scheme. The required reactive power (q) is obtained from the difference between the motor side reactive power demand and the supply side reactive power output. Shown in Equation (19), the SSSC reference voltages in α - β frame ($v_{\alpha_inj}^*, v_{\beta_inj}^*$) are computed using the desired value of reactive power that is to be supplied from the SSSC.

$$\begin{bmatrix} v_{\alpha_inj}^* \\ v_{\beta_inj}^* \end{bmatrix} = \begin{bmatrix} i_{L\alpha} & i_{L\beta} \\ -i_{L\beta} & i_{L\alpha} \end{bmatrix}^{-1} \begin{bmatrix} p = 0 \\ \bar{q}^* \end{bmatrix} \quad (19)$$

In Equation (19), setting the real power (p) equal to zero ensures that the SSSC feeds only reactive power and requires the minimal amount of energy storage on its DC bus. For voltage control, the α - β frame ($v_{\alpha_inj}^*, v_{\beta_inj}^*$) reference voltages are transformed into the abc reference frame using mathematical expressions similar to those in Equation (14).

After being transformed into the abc reference frame, these reference voltages are compared with the actual injected voltages (voltages across injection transformer, see Equation 17). The obtained difference voltage signals are compared with a triangular waveform control signal. Comparison of the difference voltage signals with the triangular waveform results in switching signals for the SSSC devices. The switching

signals ensure that actual injected voltages follow the reference injected voltages.

IV. PERFORMANCE OF DYNAMIC VAR DEVICES

The developed mathematical models of the STATCOM, SSSC, and control algorithms are used to assess the performance and effectiveness of the dynamic VAR compensation schemes. The models are developed in C, and the simulated results for a 30 HP motor are given below.

A. Results for an Induction Motor without VAR Compensation

A 60 Hz, 30 HP induction motor is simulated with the following parameters:

$$R_S = 0.2511\Omega$$

$$R_R = 0.2489\Omega$$

$$L_S = 0.439H$$

$$L_R = 0.439H$$

The three-phase voltage supply has a peak amplitude of 587.0 V. The inertia of the load is set to be 0.700 kg-m². Fig. 3(a) shows the starting speed of the induction motor. Without compensation, the motor needs approximately 0.89 seconds to start. Fig 3(b) shows the phase a voltage appearing at the motor terminal. A significant amount of voltage sag is observed until the motor has fully started.

Fig. 4 shows the phase a line current when the motor is started. A large current inrush is present which is capable of disturbing the supply system.

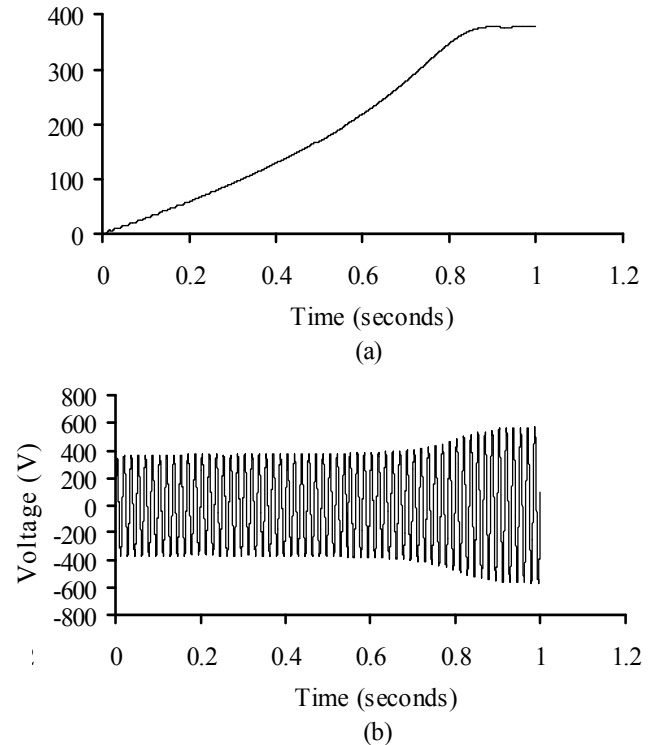


Fig. 3. Starting response of high power induction motor without compensation (a) speed of the induction motor and (b) phase a voltage v_{sa} across the motor winding.

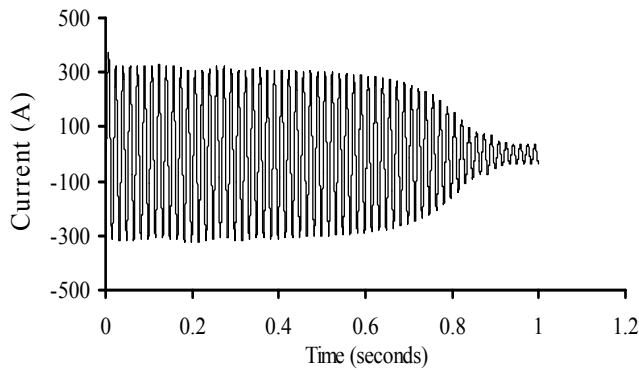


Fig. 4. Starting current for the phase a winding (i_{L_a}) of a high power induction motor without any compensation.

B. Results for an Induction Motor with Shunt Compensation

The results for the shunt compensated system for the induction motor are shown below. Fig. 5(a) shows the starting speed of the shunt compensated induction motor. The motor is started at 0.1 seconds (this time is needed to charge STATCOM DC bus) and reaches the final speed at 0.76 seconds. With this scheme, the motor needs approximately 0.66 seconds to start and consequently, starts up faster than the system without compensation. Fig. 5(b) shows the phase a voltage appearing at the motor terminal. The duration of the voltage sag is reduced and causes the startup acceleration of the induction motor to increase.

Fig. 6 shows the phase a line current when the motor is started. The higher starting current produces a higher starting torque which consequently reduces the motor starting time.

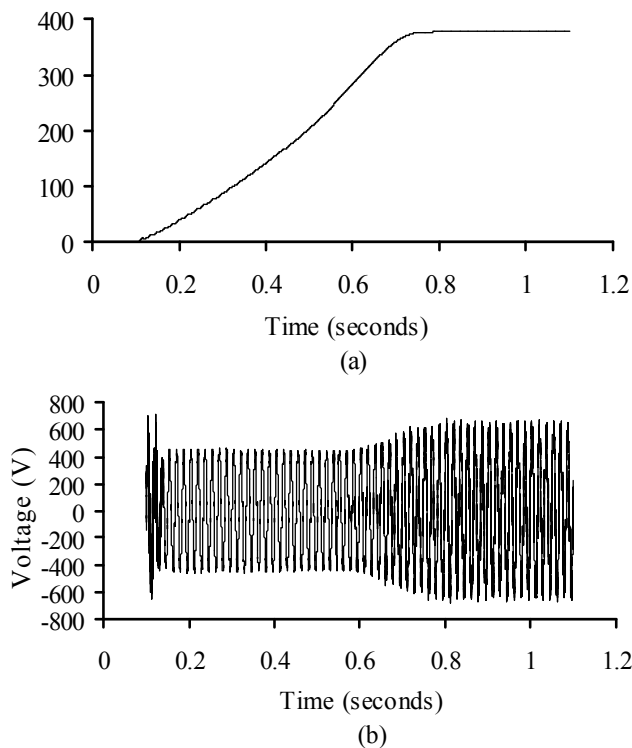


Fig. 5. Starting response of a high power induction motor with a STATCOM-based compensation technique (a) speed of the induction motor and (b) phase a voltage v_{s_a} across the motor winding.

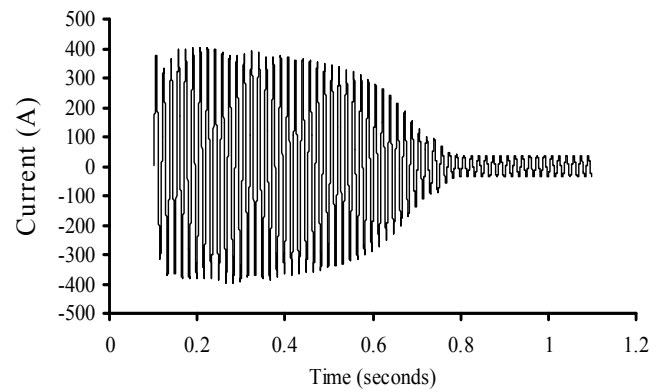


Fig. 6. Starting current for the phase a winding (i_{L_a}) of a high power induction motor with the STATCOM-based compensation technique.

C. Results for an Induction Motor with Series Compensation

The results for the series compensated system for the induction motor are shown below. Fig. 7(a) shows the starting speed of the series compensated induction motor. With this scheme, the motor needs approximately 0.56 seconds to start and consequently starts up faster than the shunt compensated system. Fig. 7(b) shows the phase a voltage appearing at the motor. The duration of the voltage sag is reduced, which raises the value of motor startup acceleration. Also, the amount of voltage sag is decreased from 200 V (without compensation) to 100 V with the series compensated system. This reduction in magnitude also contributes to reduction in the motor startup time.

Fig. 8 shows the phase a line current when the motor is started. The higher starting current produces a higher starting torque, which consequently reduces the starting motor time.

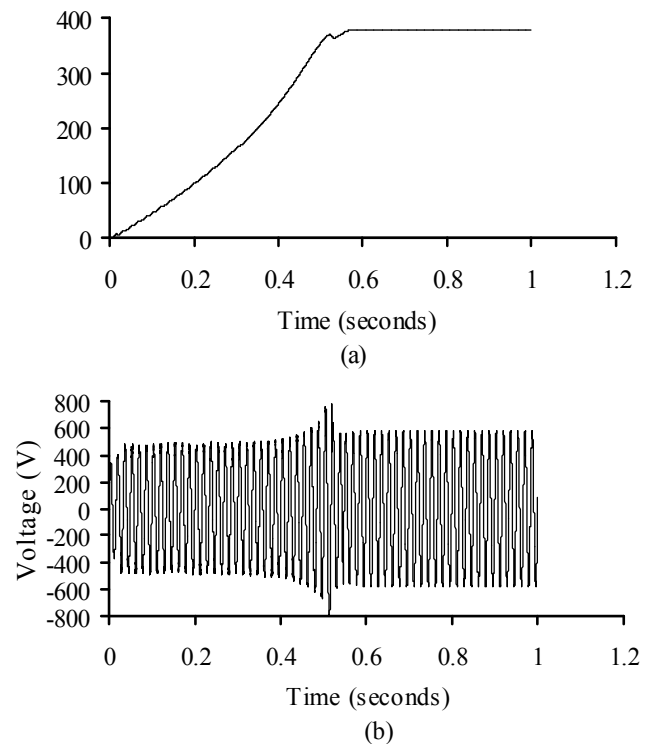


Fig. 7. Starting response of a high power induction motor with the SSSC-based compensation technique (a) speed of the induction motor and (b) phase a voltage v_{s_a} across the motor winding.

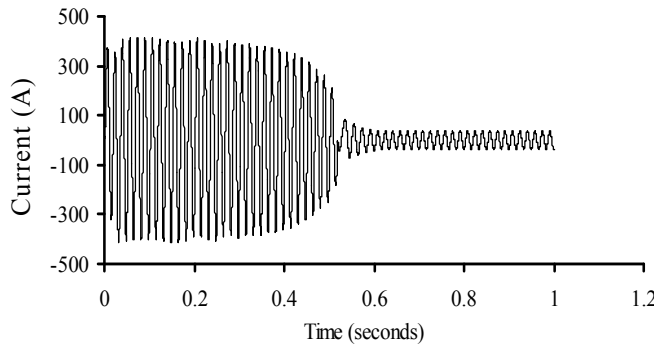


Fig. 8. Starting current for the phase a winding (i_{La}) of a high power induction motor with SSSC-based compensation technique.

Fig. 9 shows the injected voltage, which is added with the PCC supply, thereby raising the voltage imposed across the motor windings. With the VC-VSI based series compensation scheme, the injected voltage drops to a significantly low value as soon as motor starts and reaches its final speed. Therefore, as compared to series switched capacitor systems, series compensation not only offers superior performance but also results in a reliable and maintenance free operation.

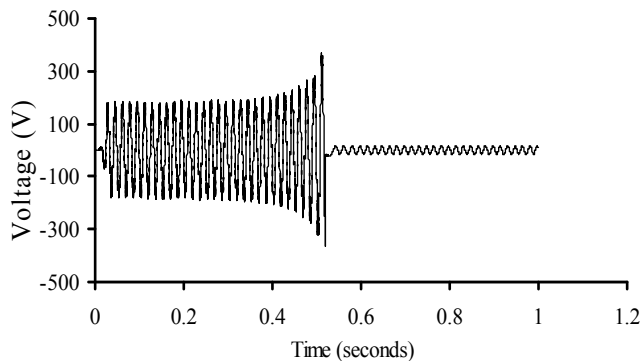


Fig. 9. Injected voltage in series with the motor.

V. CONCLUSION

Two novel dynamic shunt and series compensation schemes for motor starting are presented in this paper. Instantaneous reactive power theory is utilized to obtain an improved control algorithm for the voltage source inverter operating in current control mode for shunt compensation and in voltage control mode for series compensation. Mathematical models for both compensation schemes are derived and coded in C to obtain simulation results. The simulated results reveal that the proposed compensation techniques are found to be effective as they minimize the problem of voltage sag and current inrush. It is observed that the compensation techniques result in a substantial rise in the startup acceleration while reducing the overall startup time of the high power induction motor.

VI. REFERENCES

- [1] FERC Staff Report, "Principles for efficient and reliable reactive power supply and consumption," Feb. 2005.
- [2] A. Bendre, D. Divan, W. Kranz, and W. E. Brumsickle, "Are voltage sags destroying equipment?," *IEEE Industry Applications Magazine*, vol. 12, no. 4, pp. 12-21, Jul./Aug. 2006.
- [3] B.-S. Chen and Y.-Y. Hsu, "A minimal harmonic controller for a STATCOM," *IEEE Trans. Industrial Electronics*, vol. 5, pp. 655-664, Feb. 2008.
- [4] K. Li, J. Liu, Z. Wang, and B. Wei, "Strategies and operating point optimization of STATCOM control for voltage unbalance mitigation in three-phase three-wire systems," *IEEE Trans. Power Delivery*, vol. 22, no. 1, pp. 413-422, Jan. 2007.
- [5] S.-J. Tsai and Y. Chang, "Dynamic and unbalance voltage compensation using STATCOM," in *Proc. IEEE Power and Energy Society General Meeting*, Jul. 2008.
- [6] B. N. Singh, B. Singh, A. Chandra, P. Rastgoufard, and K. Al-Haddad, "An improved control algorithm for active filters," *IEEE Trans. Power Delivery*, vol. 22, no. 2, pp. 1009-1020, Apr. 2007.
- [7] P. Zuniga-Haro and J. M. Ramirez, "Multipulse VSC based SSSC," in *Proc. IEEE Power and Energy Society General Meeting*, Jul. 2008.